Research Article | Vol. 25, No. 4 | 20 Feb 2017 | OPTICS EXPRESS 3694

Optics EXPRESS

Radio-over-fiber linearization with optimized genetic algorithm CPWL model

CARLOS MATEO,* PEDRO L. CARRO, PALOMA GARCÍA-DÚCAR, JESÚS DE MINGO, AND ÍÑIGO SALINAS

Department of Electronic Engineering and Communications, Aragon Institute of Engineering Research (I3A), University of Zaragoza, Zaragoza, 50.018, Spain
**cmperez@unizar.es*

Abstract: This article proposes an optimized version of a canonical piece-wise-linear (CPWL) digital predistorter in order to enhance the linearity of a radio-over-fiber (RoF) LTE mobile fronthaul. In this work, we propose a threshold allocation optimization process carried out by a genetic algorithm (GA) in order to optimize the CPWL model (GA-CPWL). Firstly, experiments show how the CPWL model outperforms the classical memory polynomial DPD in an intensity modulation/direct detection (IM/DD) RoF link. Then, the GA-CPWL predistorter is compared with the CPWL model in several scenarios, in order to verify that the proposed DPD offers better performance in different optical transmission conditions. Experimental results reveal that with a proper threshold allocation, the GA-CPWL predistorter offers very promising outcomes.

OCIS codes: (060.5625) Radio frequency photonics; (060.2330) Fiber optics communications.

References and links

1. T. Pfeiffer, "Next generation mobile fronthaul architectures," in Optical Fiber Communications Conf. 2015 (Optical Society of America, 2015), paper M2J.7.
2. Y. Xu, X. Li, J. Yu, and G. Chang, "Simple and reconfigured single-sideband OFDM RoF system," Opt. Express **24**(20), 22830–22835 (2016).
3. D. Waken, A. Nkansah, and N. J. Gomes, "Radio over fiber link design for next generation wireless systems," J. Lightwave Technol. **28**(16), 2456–2464 (2010).
4. S. E. Alavi, M. R. K. Soltanian, I. S. Amiri, M. Khalily, A. S. M. Supaat, and H. Ahmad, "Towards 5G: a photonic based millimeter wave signal generation for applying in 5G access fronthaul," Scientific Reports, **6**, 19891 (2016).
5. J. Zhou, S. Fu, F. Luan, J. H. Wong, S. Aditya, P. P. Shum, and K. E. K. Lee, "Tuneable multi-tap bandpass microwave photonic filter using a windowed Fabry-Pérot filter-based multi-wavelength tuneable laser," J. Lightwave Technol. **29**(22), 3381–3386 (2011).
6. N. Alic, "Cancellation of nonlinear impairments in fiber optic transmission systems," in Optical Fiber Communications Conf. 2016 (Optical Society of America, 2016), paper Tu2E.1.
7. J. Amstrong, "OFDM of optical communications," J. of Lightwave Technology **27**(3), 189–204 (2009).
8. Y. Pei, K. Xu, J. Li, A. Zhang, Y. Dai, Y. Ji, and J. Lin, "Complexity-reduced digital predistortion for subcarrier multiplexed radio over fiber systems transmitting sparse multi-band RF signals," Opt. Express **21**(3), 3708–3714 (2013).
9. C. Han, S. Cho, H. S. Chung, and J. H. Lee, "Linearity improvement of directly-modulated multi-IF-over-fiber LTE-A mobile fronthaul link using shunt diode predistorter," in European Conference and Exhibition on Optical Communications 2015 (Optical Society of America, 2015), paper We.4.4.4.
10. A. Zhu, "Decomposed vector rotation-based behavioral modeling for digital predistortion of RF power amplifiers," IEEE Trans. Microwave Theory Tech. **63**(2), 737–744 (2015).
11. P. Guo, X. Wang, and Y. Han, "The enhanced genetic algorithms for the optimization design," in Proc. of IEEE Conference on Biomedical Engineering and Informatics 2010 (IEEE, 2010), pp. 2990–2994.
12. A. Zhu, P. J. Draxler, J. J. Yn, T. J. Brazil, D. F. Kimball, and P. M. Asbeck, "Open-loop digital predistorter for RF power amplifiers using dynamic deviation reduction-based volterra series," IEEE Trans. Microwave Theory Tech. , **56**(7), 1524–1534 (2008).
13. L. Ding, G. Tong Zhou, D. T. Morgan, Z. Ma, J. S. Kenney, J. Kim, and C. R. Giardina, "A robust digital baseband predistorter constructed using memory polynomials," IEEE Trans. Commun. **52**(1), 159–165 (2004).
14. L. O. Chua, and S. M. Kang, "Section-wise piecewise-linear functions: canonical representation, properties and applications," Proc. of the IEEE **65**(6), 915–929 (1977).
15. 3GPP TSGRAN, "User equipment (UE) radio transmission and reception (FDD)," Technical Specification ETSI TS136.101 V9.4.0 (2010).

#280539 https://doi.org/10.1364/OE.25.003694
Journal © 2017 Received 10 Nov 2016; revised 23 Dec 2016; accepted 27 Dec 2016; published 10 Feb 2017

Optics EXPRESS

16. M. Aziz, M. Rawat, and F. M. Ghannouchi, "Low complexity distributed model for the compensation of direct conversion transmitter's imperfections," IEEE Trans. Broadcast. **60**(3), 568–574 (2014).
17. Cox, C. H. III, Betts, G. E. and Johnson, L. M., "An analytic and experimental comparison of direct and external modulation in analog fiber-optic links, " IEEE Trans. Microwave Theory Tech. , **38**(5), 501–509 (1990).

1. Introduction

Nowadays, due to the increasing demand of Information and Communication Technology (ICT) services, new architectures have been developed in order to concentrate signal processing in the same Baseband Unit (BBU), such as Cloud Radio Access Network (C-RAN) [1]. In addition, Radio-over-Fiber (RoF) connections are becoming more important because of their well-known benefits, such as extremely broad bandwidth, low loss transmission, immunity to electromagnetic interference [2–4], and potential compatibility to several microwave photonic processing techniques [5]. However, RoF transmissions are analog systems, and thus susceptible of nonlinear distortions by electrical-to-optical and optical-to-electrical conversions, as well as the fiber dispersion [6]. This issue, together with the power amplifier (PA) situated at the Remote Radio Head (RRH) side, distort the signal producing a spectral regrowth in adjacent frequency bands, known as adjacent channel interference (ACI). Current standards, such as Long Term Evolution (LTE) or Long Term Evolution-Advanced (LTE-A), are based on orthogonal frequency division multiplexing (OFDM), which provides major advantages in mitigating wireless channel impairments. In addition, in optical communications, OFDM can tolerate various fiber dispersion [7]. However, it is especially vulnerable to these distortions due to its high peak-to-average power ratio (PAPR) in its signal envelope.

Both photonic and electrical methods have been developed in order to address these RoF system distortions [8, 9], being digital predistortion (DPD) one of the most effective with high flexibility and simple operation. Most DPD methods are based on Volterra series, which provide a general way to model a non-linear system with memory effects. The main disadvantage of memory polynomial models is that they suffer from numerical instability when the model order increases, offering unsatisfactory results. A DPD model based on canonical piece-wise-linear (CPWL) functions is presented in [10], in which several modifications have been carried out in order to satisfy modeling conditions: in the discrete time domain, taking into account static nonlinearity and memory effects, linear in parameters and dealing with complex signals. Until now, several DPD have been proposed and widely used for wireless systems. However, there have no reports to apply CPWL models in IM/DD RoF systems.

In this work, we present an optimized version of the CPWL model. The advantage of this model relies on the influence of the thresholds in its performance. To address this fact, a genetic algorithm (GA) has been used to determine their optimum values [11], improving the fitness and offering better performance. The experiments have been carried out in a RoF LTE mobile fronthaul link, whose optical parameters have been changed in order to verify the DPD model adaptability to different transmission conditions.

This article is organized as follows. Section 2 presents the proposed model. Experimental results without optimization in a simple setup are shown in Section 3. Section 4 presents the experimental results after optimization process in several optical scenarios, and finally, conclusions are stated in Section 5.

2. Proposed models

2.1. Volterra model

The classical polynomial model based on truncated Volterra series has been deeply studied along the literature, and is defined as

Optics EXPRESS

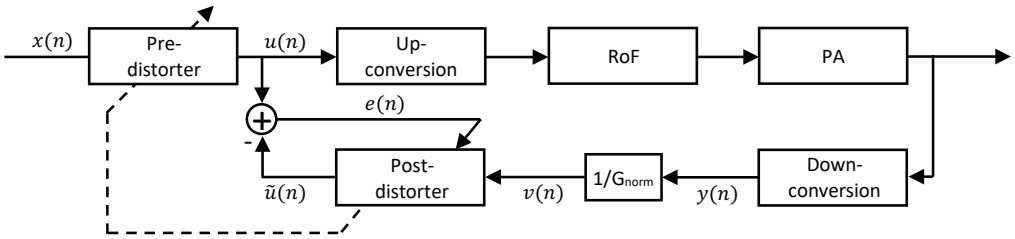

Fig. 1. Digital Predistorter schematic in a RoF mobile-fronthaul system.

$$u(n) = \sum_{p=1}^{N} \sum_{m=0}^{M} a_{pm} x(n-m)|x(n-m)|^{p-1}, \tag{1}$$

where N is the non-linear order, M is the memory depth, $x(n)$ and $u(n)$ are the predistorter baseband input and output signals, respectively, and a_{pm} are the model coefficients. The indirect-learning structure used in this work (see Fig. 1) estimates the DPD coefficients. They are calculated in a first stage in the feedback path (post-distorter), whose input is $v(n)$ and is defined as $v(n) = y(n)/\mathrm{G_{norm}}$, with $\mathrm{G_{norm}} = G_{RoF}^{lin} = \alpha \cdot G_{RoF}$, where G_{RoF}^{lin} is the linearized RoF mobile-fronthaul complex gain, α the gain factor and G_{RoF} the complex gain without linearization defined as $G_{RoF} = max\left[|y(n)|\right] / \max\left[|x(n)|\right]$. The factor α is used to compensate the gain reduction due to the linearization process. The DPD performance can be improved by carefully adjusting this factor, as long as the DPD model remains stable [12]

A more detailed description of this well-known method and how to obtain the input signal matrix expression, as well as the coefficient vector, can be found in [13].

This model can fit the non-linearity and the memory effects caused both by the RoF mobile-fronthaul link and the power amplifier. However, they may be not very accurate to model the spectral regrowth in adjacent frequency bands, and therefore DPD identification may be unsatisfactory.

2.2. CPWL model

The canonical piecewise-linear function (CPWL) was proposed by Chua [14] as a simple structure capable of represent a wide range of continuous nonlinear functions with high precision, defined as

$$u(n) = \sum_{m=0}^{M} a_m x(n-m) + b + \sum_{k=1}^{K} c_k \left| \sum_{m=0}^{M} a_{km} x(n-m) - \beta_k \right|, \tag{2}$$

where $x(n)$ and $u(n)$ are the DPD baseband input and output signals, respectively. K is the partition number and β_k is the threshold that defines the partition boundary. M represents the memory depth and a_m, b, c_k and a_{km} are the coefficient vectors. However, this CPWL model cannot be directly employed in DPD identification because it does not satisfy the DPD modeling conditions. Moreover, it is necessary to make some modifications in order to deal with complex signals, as well as to take into account the interactions of the present and past samples. A modified model using a decomposed vector rotation technique is proposed in [10], which is defined as

Optics EXPRESS

$$
\begin{aligned}
u(n) = & \sum_{m=0}^{M} c_m x(n-m) && \text{linear} \\
& + \sum_{k=1}^{K} \sum_{m=0}^{M} c_{km,1} \, ||x(n-m)| - \beta_k| \, e^{j\theta(n-m)} && \text{1st-order basis} \\
& + \sum_{k=1}^{K} \sum_{m=0}^{M} c_{km,21} \, ||x(n-m)| - \beta_k| \, e^{j\theta(n-m)} \cdot |x(n)| && \text{2nd-order type-1} \\
& + \sum_{k=1}^{K} \sum_{m=0}^{M} c_{km,22} \, ||x(n-m)| - \beta_k| \cdot x(n) && \text{2nd-order type-2} \\
& + \sum_{k=1}^{K} \sum_{m=0}^{M} c_{km,23} \, ||x(n-m)| - \beta_k| \cdot x(n-m) && \text{2nd-order type-3} \\
& + \sum_{k=1}^{K} \sum_{m=0}^{M} c_{km,24} \, ||x(n)| - \beta_k| \cdot x(n-m) && \text{DDR term-1} \\
& + \cdots ,
\end{aligned}
\tag{3}
$$

where K is the number of partitions and β_k is the threshold that defines the boundary of the partition, whereas M represents the memory depth. $x(n)$ and $u(n)$ are the predistorter baseband input and output signals, respectively. c_m, $c_{km,1}$, $c_{km,21}$, $c_{km,22}$, $c_{km,23}$ and $c_{km,24}$ are the coefficient vectors. The method to obtain these coefficient vectors is analogous to the Volterra model. Balancing the performance and the implementation complexity, in this work a truncated version of this model has been used, taking into account only up to 2nd-order type-2, in order to minimize the coefficient number. This model is defined as

$$
\begin{aligned}
u(n)\,|_{CPWL} = & \sum_{m=0}^{M} c_m x(n-m) \\
& + \sum_{k=1}^{K} \sum_{m=0}^{M} c_{km,1} \, ||x(n-m)| - \beta_k| \, e^{j\theta(n-m)} \\
& + \sum_{k=1}^{K} \sum_{m=0}^{M} c_{km,21} \, ||x(n-m)| - \beta_k| \, e^{j\theta(n-m)} \cdot |x(n)| \\
& + \sum_{k=1}^{K} \sum_{m=0}^{M} c_{km,22} \, ||x(n-m)| - \beta_k| \cdot x(n).
\end{aligned}
\tag{4}
$$

2.3. *Threshold optimization with genetic algorithms*

An uniform threshold allocation along the signal amplitude has been set in [10], but it might not be the suitable solution due to the relationship between the system performance and its parameters. It is important to choose properly these values in order to obtain a better behavioral model. Along the literature detailed investigations on the threshold influence in the CPWL model behavioral are not reported yet.

In this work we propose the use of the GA algorithm in order to determine the optimum allocation of the DPD model thresholds (see Fig. 2). GA is a powerful stochastic algorithm based on the principles of natural selection. This algorithm maintains a population of individuals and probabilistically modifies it by some genetic operators such as selection, crossover and mutation, in order to seek an optimal solution. After several iterations (generations), the algorithm converges to the optimal solution.

Firstly, it is necessary to determine a set of limits which determine the segments where the GA will set the initial threshold population. In this work we have chosen a logarithmic initial limit allocation due to the form of the AM/AM DPD curve needs more thresholds for high input signal envelopes than in the linear zone. Once the limits are stablished, a random threshold population (with 50 individuals) is created within these limits. Each individual of this population is evaluated with the fitness function value φ. In this work, we have made use of the Adjacent Channel Power Ratio (ACPR) as the fitness function because in a linearization process we seek

Optics EXPRESS

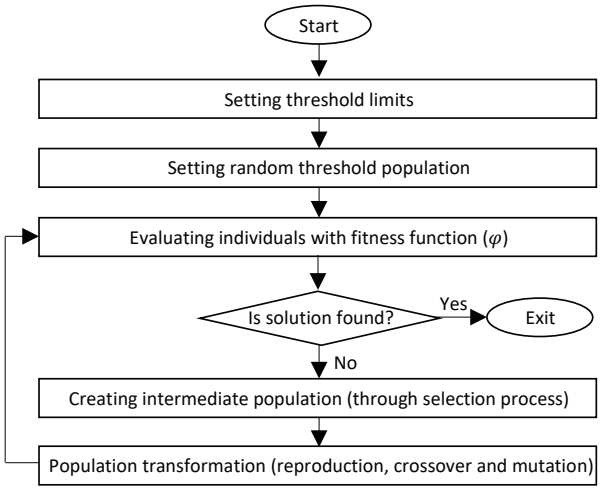

Fig. 2. Genetic algorithm threshold optimization diagram.

to reduce the spectral regrowth:

$$\varphi_{ACPR} = \min_{m=1,2}\left[10\log_{10}\frac{\int_{(adj\_band)m} Y(f)df}{\int_{(band)} Y(f)df}\right], \tag{5}$$

where $Y(f)$ is the output signal power spectral density. Once the fitness function has been evaluated for each individual, the algorithm has to decide if the process has ended. This occurs when it has converged to the best solution (the minimum value of the fitness function (ACPR)). The selection strategy is based on the fitness level, and in this work the fitness proportionate selection has been chosen. This selection function lays out a line in which each parent corresponds to a section of the line of length proportional to its scaled value. The algorithm moves along the line in steps of equal size. At each step, the algorithm allocates a parent from the section it lands on. After a new population is formed, some members of the new population are transformed by three basic operators: reproduction, crossover and mutation. The first operator only copy the selected individual from the current population into the new population without changes. In this process the number of individuals that are guaranteed to survive to the next generation is the 5% of the total population size. The crossover operator consists of combining two individuals (or parents) to form a crossover child for the next generation. This process creates a random binary vector and selects the genes where the vector is a 1 from the first parent, and the genes where the vector is a 0 from the second parent, and combines the genes to form the child. The last operator randomly generates directions that are adaptive with respect to the last successful or unsuccessful generation. The mutation chooses a direction and step length that satisfies bounds and linear constraints. This operator allows to cross the initial limits moving the thresholds to another segment that proporcionate a better solution. When the population transformation has been taken place, the individuals are evaluated again. After several generations, the algorithm converges to the best solution, which hopefully represents the optimum threshold allocation. While others algorithms could offer local solutions, one of the GA benefits is that the solution may escape from them.

Since transmission conditions depend strongly on optical parameters, the threshold optimization process changes in each scenario. Therefore, the thresholds will depend on the optic fiber length between the RRH and the BBU (L), DFB bias intensity (I_{bias}) and RF input power

Optics EXPRESS

(P_{RF}). Taking this issue into account, the Eq. (4) leads to:

$$\begin{aligned} u(n)\,|_{GA-CPWL} = & \sum_{m=0}^{M} \tilde{c}_m x(n-m) \\ & + \sum_{k=1}^{K} \sum_{m=0}^{M} \tilde{c}_{km,1} \left| |x(n-m)| - \tilde{\beta}_k(L, I_{bias}, P_{RF}) \right| e^{j\theta(n-m)} \\ & + \sum_{k=1}^{K} \sum_{m=0}^{M} \tilde{c}_{km,21} \left| |x(n-m)| - \tilde{\beta}_k(L, I_{bias}, P_{RF}) \right| e^{j\theta(n-m)} \cdot |x(n)| \\ & + \sum_{k=1}^{K} \sum_{m=0}^{M} \tilde{c}_{km,22} \left| |x(n-m)| - \tilde{\beta}_k(L, I_{bias}, P_{RF}) \right| \cdot x(n), \end{aligned} \tag{6}$$

where K is the number of partitions and $\tilde{\beta}_k$ is the optimized threshold, whereas M represents the memory depth. $x(n)$ and $u(n)$ are the predistorter baseband input and output signals, respectively. As in the CPWL model, $\tilde{c}_m$, $\tilde{c}_{km,1}$, $\tilde{c}_{km,21}$ and $\tilde{c}_{km,22}$ are the coefficient vectors for linear, 1st-order basis, 2nd-order type-1 and 2nd-order type-2 terms, respectively. The process to obtain these coefficient vectors are analogous to the previous models.

3. Experimental results without optimization

3.1. Experimental setup

The test setup used in this section to study both methods (Volterra and CPWL) is shown in Fig. 3. It consists of a directly-modulated RoF system, as well as the electrical segment at the RRH. An arbitrary signal generator (*Agilent E4438C*) is used to generate a signal composed by two LTE downlink signals (OFDM modulation) with QPSK and 16QAM subcarriers whose bandwidths are 5 and 15 MHz, respectively. The RF carrier frequencies are set at 2.6625 and 2.6825 GHz, and are within the Band 7 of the LTE standard [15]. The signals feed an electro-absorption modulator (EAM) distributed feedback laser (DFB) (*Optilab DFB-EAM-1550-12 S/N7075*) with an input RF power of 0 dBm, whose wavelength is 1550 nm. To ensure the EAM-DFB laser is not biased close to the lasing threshold level (<10 mA) and the saturation region (>100 mA), the process is carried out with a 50 mA bias intensity. The link between BBU and RRH is a single-mode fiber (SMF) with an attenuation of 0.25 dB/Km, a dispersion of 18 ps/(nm·Km) and is 10 km length. The RRH side consists of a photodetector (PD) with a responsivity of 0.9 A/W. After the optic-electric conversion, a PA (*Minicircuits ZHL-4240*) is used, with a 1-dB compression point of 26 dBm, and an approximated gain of 41.7 dB at

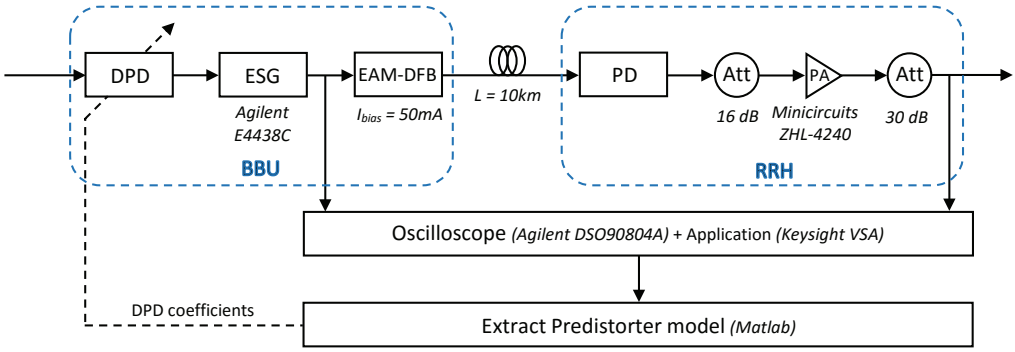

Fig. 3. Experimental setup for a directly-modulated RoF system.

Optics EXPRESS

Table 1. RoF modeling comparison between Volterra and CPWL Models in terms of NMSE and ACEPR for different Nonlinearity Orders and Memory Depths.

N	K	M	Coeff.	NMSE (dB)		ACEPR (dB)	
				Volterra	CPWL	Volterra	CPWL
7	2	0	7	−21.62	−21.60	−36.82	−37.15
13	4	0	13	−21.62	−21.62	−36.84	−36.90
19	6	0	19	−21.62	−21.62	−36.81	−36.87
7	2	1	14	−29.30	−29.32	−34.25	−40.27
13	4	1	26	−29.30	−29.47	−34.32	−42.75
19	6	1	38	−29.30	−29.48	−34.36	−42.47
7	2	2	21	−31.22	−31.24	−35.63	−45.57
13	4	2	39	−31.23	−31.51	−35.74	−49.16
19	6	2	57	−31.23	−31.55	−35.78	−49.24

the test frequencies. The setup includes a 16 dB attenuator to avoid PA damage. Finally, the output signals are captured by means of an oscilloscope (*Agilent Infiniium DSO90804A*), which measures Error Vector Magnitude (EVM) and ACPR. The model coefficients are calculated from these captured signals in a PC with *Matlab*.

3.2. RoF modeling results

The parameters for both the CPWL and the Volterra models are set to ensure the coefficient number is equal. Hence, for Volterra model the nonlinearity orders are N=7, 13 and 19; and for CPWL model the number of thresholds are K=2, 4 and 6. The memory depths are set at the same values for both models: M=0, 1 and 2. Table 1 summarizes the performance comparison of both models in terms of Normalized Mean Square Error (NMSE) and Adjacent Channel Error Power Ratio (ACEPR) [16]. Concerning to the first, Volterra and CPWL models give similar features, being CPWL model results lightly better. Regarding to the ACEPR, when the coefficient number increases, the CPWL model performance improves, reducing its value from -35.78 to -49.24 dB.

Table 2. DPD Experimental Results for both Volterra and CPWL Models in terms of NMSE and ACPR for different Nonlinearity Orders and Memory Depths.

N	K	M	Coeff.	NMSE (dB)		ACPR (dBc)			
						Band 1		Band 2	
				Volterra	CPWL	Volterra	CPWL	Volterra	CPWL
7	2	0	7	−21.27	−20.95	−33.39	−34.21	−36.87	−36.96
13	4	0	13	−21.30	−20.99	−22.03	−21.67	−22.30	−21.58
19	6	0	19	−21.31	−21.29	−20.65	−33.84	−21.73	−37.25
7	2	1	14	−26.77	−25.71	−32.97	−33.48	−34.93	−35.35
13	4	1	26	−27.10	−25.99	−27.12	−37.98	−30.46	−39.79
19	6	1	38	−27.16	−26.85	−19.30	−33.39	−25.06	−35.08
7	2	2	21	−27.70	−26.43	−37.48	−35.66	−39.79	−37.83
13	4	2	39	−28.21	−26.92	−28.10	−37.48	−31.23	−40.02
19	6	2	57	−28.32	−28.03	−18.69	−34.01	−24.83	−35.75

Optics EXPRESS

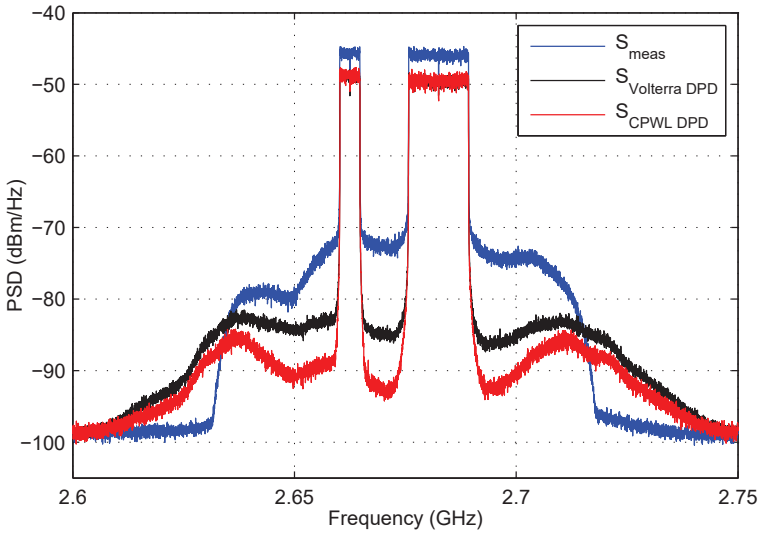

Fig. 4. Output signal PSDs without predistortion (blue) and with Volterra (black) and CPWL DPD (red) with 26 coefficients (M=1, N=13 and K=4).

3.3. *DPD identification results*

NMSE and ACPR measurements are required in order to validate the linearization performance of the Volterra and CPWL models. According to table 2, Volterra offers lightly better performance than CPWL regarding to NMSE. If the AMAM curves from both modeling and predistortion are taken into account, in modeling the nonlinear zone can be modeled with several thresholds, whereas in the DPD curve the nonlinear zone has to be modeled with only one threshold. However, in terms of ACPR, experimental results show that in most tested cases the CPWL DPD offers better features. This improvement is especially pronounced with 39 coefficients (M=2, N=13 and K=4) in Band 1, reaching an enhancement of 9.38 dB with a value of -37.48 dB. Nevertheless, the best result has been obtained for the same measurement conditions

Table 3. Transmitted Signal Power at the PA Output in both Bands without Predistortion and with Volterra and CPWL DPD for different Nonlinearity Orders and Memory Depths.

N	K	M	Coeff.	$\text{Power}_{\text{channel}}$ (dBm)			
				Band 1		Band 2	
				Volterra	CPWL	Volterra	CPWL
w/o DPD				16.18	16.18	20.61	20.61
7	2	0	7	12.68	12.67	17.04	17.05
13	4	0	13	12.78	12.78	17.19	17.19
19	6	0	19	13.28	12.81	17.64	17.16
7	2	1	14	12.90	12.94	16.92	16.95
13	4	1	26	13.23	13.01	17.15	17.08
19	6	1	38	11.22	12.83	16.42	16.80
7	2	2	21	12.82	12.97	16.99	17.09
13	4	2	39	12.82	12.76	16.97	16.96
19	6	2	57	12.63	12.82	16.78	17.01

Optics EXPRESS

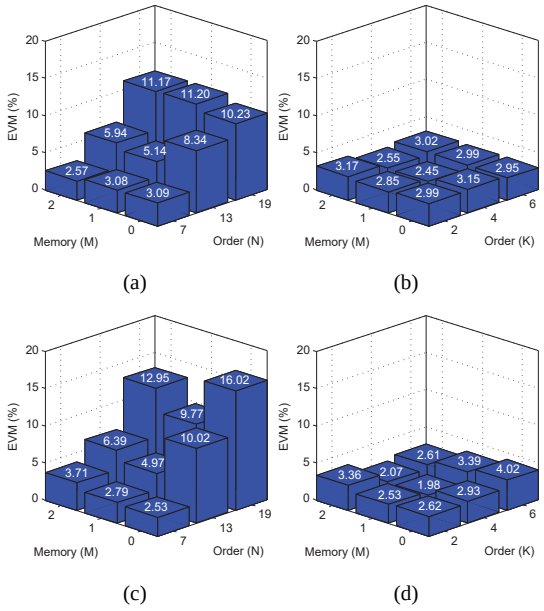

Fig. 5. EVM experimental results for different coefficient number and memory depths. (a) Band 1 with Volterra model; (b) Band 1 with CPWL model; (c) Band 2 with Volterra model and (d) Band 2 with CPWL model.

in Band 2, with an ACPR of -40.02 dB.

The linearization capacity is further confirmed by examining the output signal power spectral densities (PSD) with and without linearization process (see Fig. 4). Although both of the predistorted signals can cancel most of the intermodulation products, CPWL model offers better linearization capacity in terms of adjacent channel regrowth reduction. It can be seen that in some frequencies the spectral regrowth is higher than without the DPD. Due to the models can only reduce the spectral regrowth up to certain order, the rest of the terms are involved in produce the increment in the other orders. It can be seen as a power redistribution in the spectral domain.

The evaluation of the PA output power in both frequency bands for all predistorter under test is required due to the losses introduced by the DPD. Provided a fixed total RF input power of 0 dBm, the output power with and without the DPDs in the setup has been evaluated. The gain factor in this transmission conditions has been set at $\alpha = 1.35$ in order to compare the different coefficient number in the same conditions. Table 3 summarizes the experimental results, which are similar in all studied cases, with a power losses of approximately 3 dB.

Finally, the EVM has been evaluated in order to analyze the predistorted output signals quality related to the in-band interference. Experimental results show that with Volterra DPD only nonlinearity orders up to 7 offers good performance (see Fig. 5). However, with an order from 7 the model suffers instability due to the data matrix is ill-conditioned, thus the output signal EVM increases strongly reaching 11.20% and 16.02% in Band 1 and Band 2, respectively, offering worse results than without the DPD (8.37% in Band 1 and 8.51% in Band 2). It is remarkable that in Fig 5(d), with memory depth M=0, when the order increases, the DPD performance decreases. Although in Volterra model is much more noticeable, in CPWL model can also occur that the matrix is ill-conditioned. Thus, the pseudoinverse process and the coefficient calculation offers worse performance. Moreover, with CPWL model the measured EVM is worse than with Volterra model in 0.09 percentage points (see Figs. 5(c) and 5(d) with M=0 and 7

Optics EXPRESS

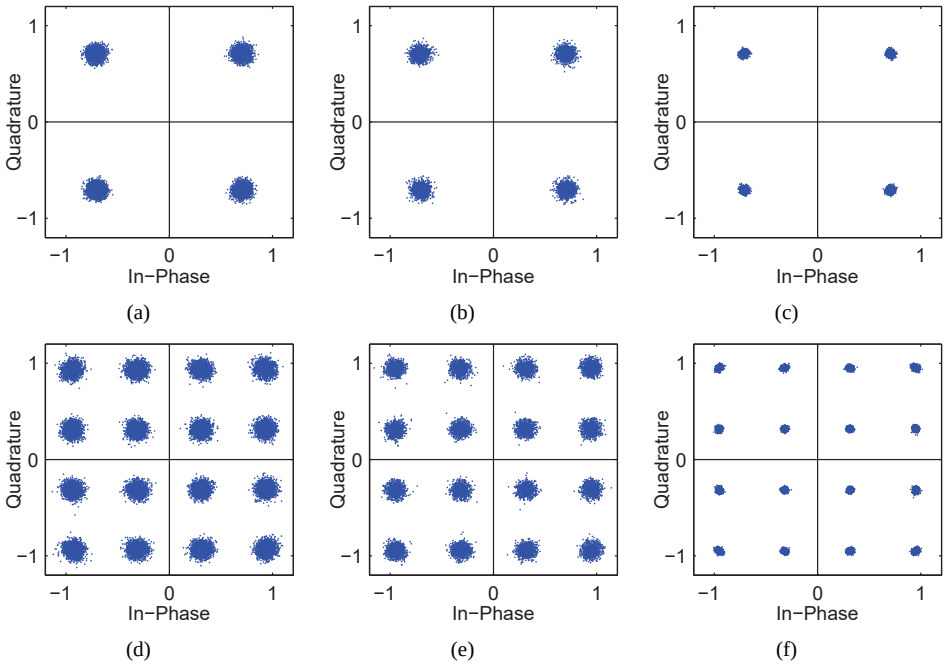

Fig. 6. Output signal constellations with 39 coefficients (N=13, K=4 and M=2). (a) Band 1 without DPD, (b) with Volterra predistorter and (c) with CPWL DPD; (d) Band 2 without DPD, (e) with Volterra predistorter and (f) with CPWL DPD.

coefficients). Taking into account that the LTE standard limits are 17.5% for QPSK and 12.5% for 16QAM [15], it is obvious that Volterra DPD does not meet the standard requirements in some cases. Concerning to the CPWL model, when a higher order is set, even though the model does not suffer from instability, only provides limited performance improvement, whereas the computational complexity increases. This conclusion is still valid in the case of the memory depth because there are not notable EVM enhancement when its value increases. Anyway, in all studied cases, the CPWL model output signals meet the standard EVM limits.

The transmitted signal constellations for both bands, with and without the DPDs are showed in Fig. 6. The Volterra DPD offers similar performance that without DPD, while the CPWL predistorters can improve the transmitted signal linearity.

4. Experimental results with threshold optimization

4.1. Experimental setup

In this section, CPWL model is compared with the proposed genetic algorithm threshold optimization model (GA-CPWL). In the previous section both methods (Volterra and CPWL) have been studied by varying the nonlinearity order and the memory depth in the same setup. The model parameters are fixed (K=6 and M=2) and the DPD performances are evaluated in several scenarios. As the model performance depends strongly on the transmission parameters, this can be accomplished by changing the DFB bias intensity, the length of the link between the BBU and the RRH or the input signal power. Hence, the setup in this section is similar to the previous one (see Fig. 3), but with theses parameters: optical fiber length (10, 15 and 20 km), DFB bias intensity (30, 50, 70 mA) and input signal power (between -8 and 4 dBm).

Optics EXPRESS

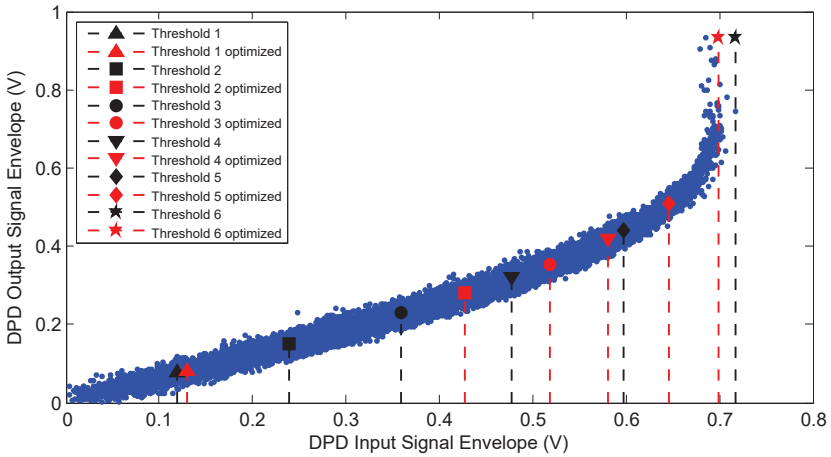

Fig. 7. Threshold allocation with (red) and without (black) optimization for input RF power of 0 dBm, I_{bias} of 50 mA and a fiber length of 10 km.

4.2. *DPD identification results*

It is first necessary to evaluate the threshold influence on the model in order to evaluate its linearization performance. According to section 3, the CPWL model uses uniform threshold allocation, but it may be unsatisfactory because the DPD AM/AM characteristic curve is not uniform, and for modeling non-linear zone will be necessary more thresholds than in the linear zone. We use the GA for seeking these optimum threshold values for each proposed scenario. Fig. 7 shows the comparative overview between CPWL and GA-CPWL models over the AM/AM DPD response with an input RF power of 0 dBm, 10-km fiber length and 50 mA bias intensity. In the linear zone the optimized threshold allocation tends to go to non-linear area, whereas the opposite happens in the non-linear zone, especially with the sixth threshold. In order to analyze their dependence on input RF power, Fig. 8 shows the fourth, fifth and sixth threshold allocation

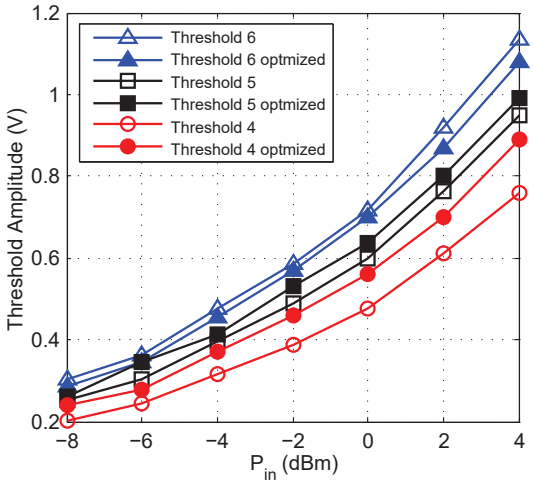

Fig. 8. Threshold amplitudes for several input signal powers with and without optimization process (L = 10 km and I_{bias} = 50 mA).

Optics EXPRESS

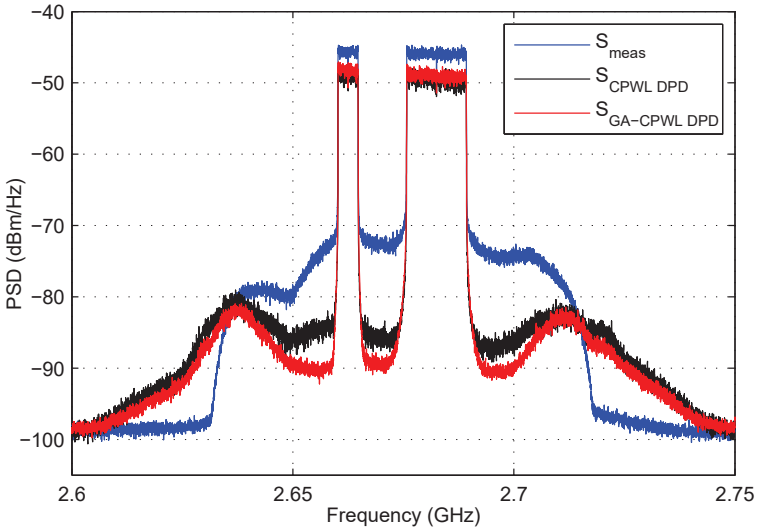

Fig. 9. Output signal PSDs without predistortion and with CPWL and GA-CPWL DPDs with 0 dBm RF input power, 10 km fiber length and 50 mA bias intensity.

with and without the optimization process. The optimized fourth and fifth threshold values are higher than their respective ones without optimization for all input RF powers. On the other hand, the optimized sixth threshold obviously offers a lower value than without optimization.

As far as distortion is concerned, ACPR provides a figure-of-merit for the DPD model performance. Fig. 9 shows the predistorted signal power spectral densities with an input power of 0 dBm and 50 mA bias intensity, as well as the output signal without DPD. Although both predistorted signals can mitigate most of the spectral regrowth, GA-CPWL model can achieve better results in terms of adjacent channel power reduction. In this case the same happens than in Fig. 4. In some frequencies the spectral regrowth is higher than without the DPD.

Moreover, ACPR has been evaluated for all proposed transmission conditions and the experimental results are summarized in Fig 10. The performance without optimization with both 5 and 15 MHz signals are similar. Moreover, with the most unfavorable setup (Figs. 10(e) and 10(f)) the performance gets worse with the CPWL model, as well as with GA-CPWL due to the high dispersion produced by the optical fiber, along with the high input power levels and 70 mA bias intensity of 70 mA (close to the nonlinear region) produce the models do not work properly. It is remarkable that the ACPR improves with the GA-CPWL model in all studied cases, being the best outcome for the 5 MHz signal with L = 20 km, I_{bias} = 50 mA and P_{RF} = 4 dBm scenario (see Fig. 10(c)) with and enhancement of 5.67 dB.

EVM experimental results for an input signal power of 4 dBm are summarized in Fig. 11, where the higher bias intensity and fiber length, the larger EVM values. On the one hand, with a high bias intensity the photodetector is more sensitive to nonlinearities. On the other hand, with higher fiber lengths the dispersion strongly concerns in the model performance, in addition to increasing the link losses. The EVM reduces its value with both models regarding to the case without DPD, being this reduction more significant with the proposed model. On the one hand, with the 5 and 15 MHz signals (L = 20 km and I_{bias} = 70 mA) the GA-CPWL model reaches an improvement of 13.56 and 33.93 percentage points, respectively, regarding to the scenarios without DPD. On the other hand, the comparison between CPWL and GA-CPWL offers an enhancement with the proposed model of 3.91 and 7.51 percentage points, respectively. In Figs. 11(e) and 11(f) (bias intensity of 50 mA and fiber length 15 km) the EVM measurements with

Optics EXPRESS

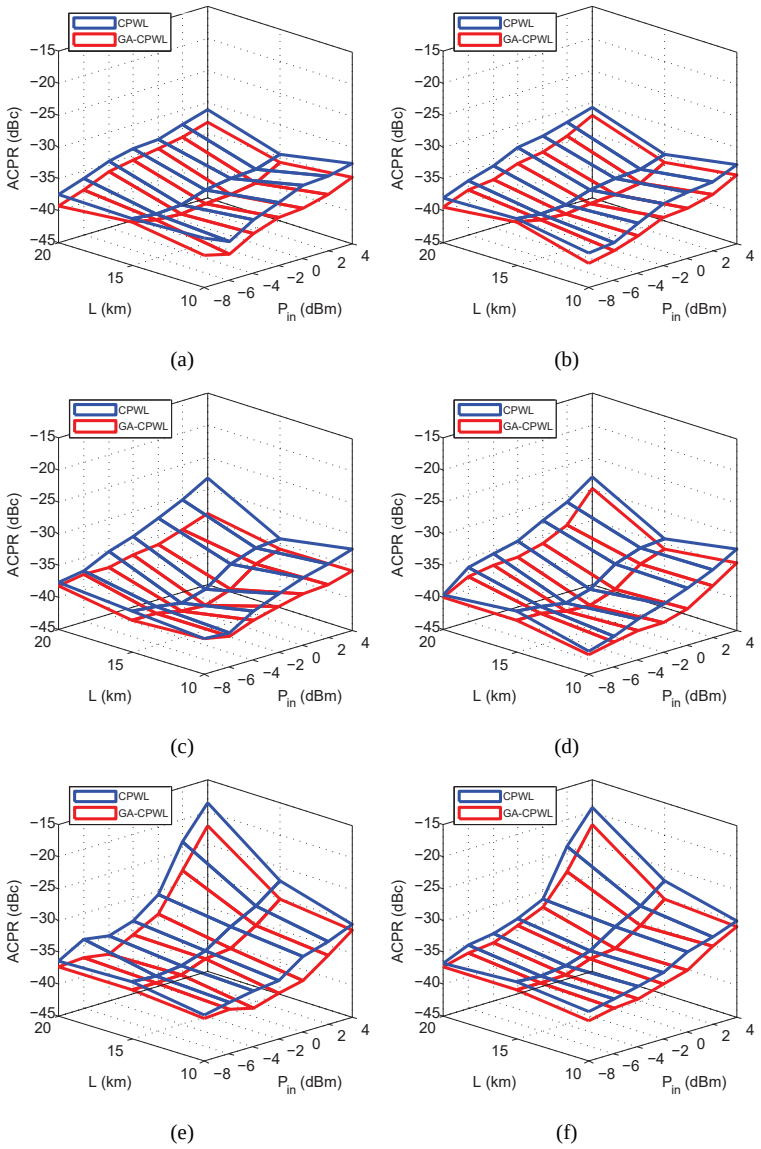

Fig. 10. ACPR experimental measurements for all studied scenarios. (a) 5 MHz and I_{bias} = 30mA; (b) 15 MHz and I_{bias} = 30mA; (c) 5 MHz and I_{bias} = 50mA; (d) 15 MHz and I_{bias} = 50mA; (e) 5 MHz and I_{bias} = 70mA and (f) 15 MHz and I_{bias} = 70mA.

GA-CPWL is worse than with current CPWL. As in Fig. 5, it may be produced by the noise present in the experimental setup (the increase is only 0.28 percentage points). Moreover, GA-CPWL model gives EVM values that meet the standard requirements, while CPWL model does not meet the standard EVM limits (see Fig. 11(e)) [15].

EVM values against the RF input power are illustrated in Fig. 12. Given a threshold by the GA-CPWL model with an RF input power of 4 dBm, the proposed model is capable of improving the RF input power tolerance by greater than 6 dB in both bands. In contrast, the enhancement does not reach 5 dB with the CPWL model.

The RoF link gain has been evaluated in all proposed scenarios. In [17] the link gain is defined

Optics EXPRESS

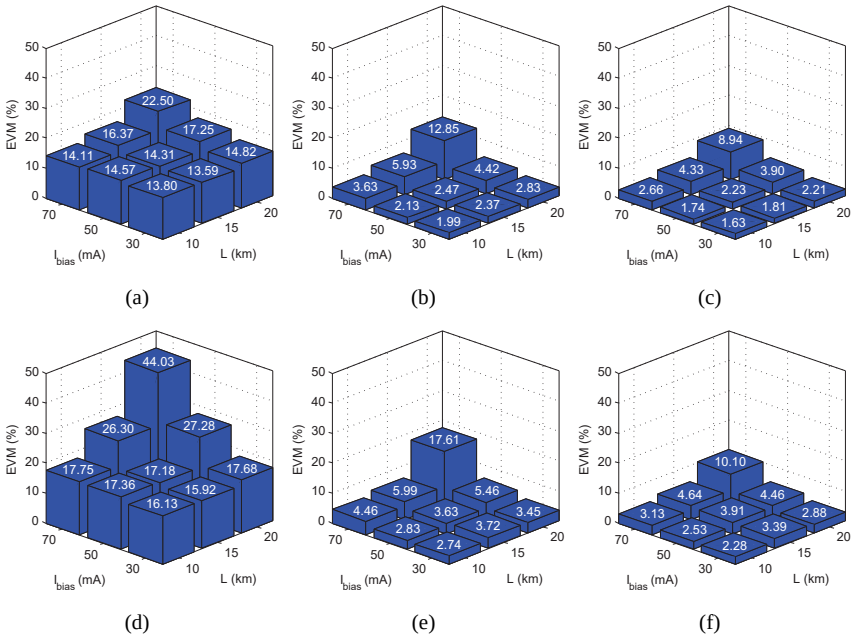

Fig. 11. EVM experimental results for an input signal power of 4 dBm. (a) 5 MHz without DPD; (b) 5 MHz DPD without optimization; (c) 5 MHz with optimization; (d) 15 MHz without DPD; (e) 15 MHz DPD without optimization and (f) 15 MHz with optimization.

as the relation between the RF output power from the optical-to-electronic converter and the RF input power to the electronic-to-optical converter. In this case we have to take into account the power amplifier situated at the RRH side as a part of the transmission chain. Thus, the overall RoF link gain is mainly dependent on the DFB laser conversion efficiency, the photodetector and the PA, as well as the losses introduced by the optical fiber:

$$\mathsf{G}_{\text{norm}} = G_{RoF}^{lin} = \alpha \cdot G_{RoF} = \alpha \cdot \frac{P_o}{P_i} = \alpha \cdot \frac{\eta_{LD}^2 \Re^2}{L_{opt}^2} \cdot G_{PA} \cdot L_{att-16dB} \cdot \frac{Z_{out}}{Z_{in}}, \qquad (7)$$

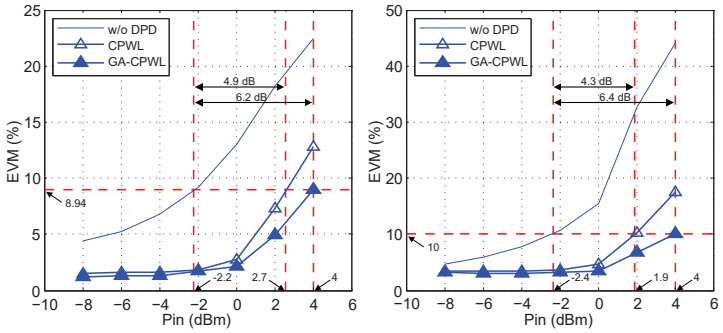

Fig. 12. EVM performance against input signal power for a length of 20 km and 70 mA bias intensity: (a) 5 MHz and (b) 15 MHz bandwidth signals.

Optics EXPRESS

Table 4. Experimental Gain Measured for all Studied Scenarios with a Fiber Length of 10 km.

I_{bias}	P_i (dBm)	G_{RoF}^{lin} (dB)			
		Band 1		Band 2	
		CPWL	GA-CPWL	CPWL	GA-CPWL
30mA	-8	11.93	12.45	15.97	16.50
	-2	7.79	8.86	11.80	12.80
	4	2.43	3.34	6.59	7.37
50mA	-8	13.59	14.17	18.15	18.69
	-2	9.00	9.93	13.04	13.99
	4	3.76	4.71	7.75	8.73
70mA	-8	11.44	12.52	15.91	16.94
	-2	6.78	8.86	10.90	11.68
	4	−1.94	1.43	3.89	5.37

where P_o and P_i are the output and input RF power, respectively. α is the gain factor, η_{LD} is the DFB slope efficiency (W/A), $\Re$ is the photodiode responsivity (A/W), L_{opt} is the optical link loss, G_{PA} the power amplifier gain and $L_{att-16dB}$ the attenuation between the PD and the PA. Z_{out} and Z_{in} are the input and output impedances, respectively.

The experimental results in terms of RoF gain are gathered in Table 4. The DPD performance of the proposed model GA-CPWL allows to set a higher value of the gain factor α (for CPWL α = 1.2 and for GA-CPWL α = 1.25). In this case this factor is lower than in the previous Section because now the transmission parameters change and in some cases these are the maximum values that work properly. With a fixed bias intensity, the higher RF input power, the lower RoF gain due to the nonlinearities produced by the DFB and the PA. When the RF input power is fixed and the bias intensity increases the RoF gain raises. However, with 70 mA bias intensity the RoF gain decreases due to the photodetector saturation. Furthermore, when the system is nonlinear the power is redistributed in adjacent bands. Thus, the overall output power is high and the power into the bands decreases.

5. Conclusion

In this work, a new optimized version of the CPWL model based on the genetic algorithm has been presented (GA-CPWL). The main idea is to optimize the threshold model with a properly allocation, reaching a better performance in DPD identification. The CPWL model has been compared with the traditional model based on a polynomial Volterra structure in the same scenario under model parameters variation. After the optimization process, the GA-CPWL model has been evaluated and compared with the current CPWL, with the model parameters fixed in several transmission conditions varying the DFB bias intensity, the RF input power and the optical fiber length. Experimental results reveal that the proposed model offers better accuracy, not only improves the ACPR and the EVM, but also the RF output signal power in both bands.

Funding

Spanish MINECO (TEC2014-58341-C4-2-R within FEDER); Diputación General de Aragón (GCM T97).